SINGLE-STEP IN SITU SEED-MEDIATED BIOGENIC SYNTHESIS OF Au, Pd AND Au-Pd NANOPARICLES BY *Etlingera elatior* LEAF EXTRACT

Sze-Ting Wong[a], Mustaffa Shamsuddin[a,b,*], Abdolhamid Alizadeh[b,c,*], Yeoung-Sang Yun[d].

[a]*Department of Chemistry, Faculty of Science, Universiti Teknologi Malaysia, 81310 UTM Skudai, Johor, Malaysia.*
[b]*Ibnu Sina Institute for Fundamental Science Studies, Universiti Teknologi Malaysia, 81310 UTM Skudai, Johor, Malaysia.*
[c]*Department of Chemistry & Nanoscience and Nanotechnology Research Center (NNRC), Razi University, Kermanshah 67149, Iran.*
[d]*Environmental Biotechnology National Research Laboratory,Department of BIN Fusion Technology, Chonbuk National University, Jeonju 561-756, Republic of Korea.*

** Corresponding Author(s): E-mail address: mustaffas@utm.my; mustaffa@kimia.fs.utm.my; ahalizadeh2@hotmail.com. Tel: +607 5534515*

ABSTRACT

The rapid formation of stable Au-Pd bimetallic nanospheres are based on a single-step, seed-mediated, growth method using *Etlingera elatior* leaf extract as a reducing, stabilizing and capping agent. The success of this synthesis is attributed to reduction potential difference of Au and Pd, where Pd initially form seeds in the reaction mixture, followed by growth of Au around the Pd seeds forming Au-Pd bimetallic nanoparticles. Consequently, monometallic Au nanoparticles with mixtures of shapes can be well controlled. The used of *Etlingera elatior* as a reducing agent is a simple one-pot environmentally friendly reaction, non-toxic and safe method without the need of additional surfactant, capping or stabilizing agent. The synthesized Au-Pd, Au and Pd nanoparticles were characterized via UV-vis, FT-IR, XRD, CV, TEM and EDX analysis. TEM analysis revealed that Au-Pd nanoparticles consisted of only nanospheres with mean size of 17.8 ± 9.9 nm, as opposed to the Au nanoparticles that have mixtures of anisotropic nanoshapes with mean size of 15.8 ± 6 nm. FTIR spectroscopic analysis of the biosynthesized Au, Pd and Au-Pd nanoparticles confirmed the surface adsorption of the bioactive components in the leaf extract that acted as the reducing agent and stabilizer for the metal nanoparticles.

Keywords: Biosynthesis, palladium, gold, nanoaparticles, *Etlingera elatior*.

1. INTRODUCTION

Nowadays, bimetallic nanoparticles derived from various noble metals are of extensive scientific and technological interest due to their unique and tailored properties for various applications in medicine, electronics, optical, materials and catalysis[1-3]. Recently, efforts to prepare uniform shapes nanoparticles have been focused on the seed-mediated growth techniques. Mirkin and co-workers had demonstrated the synthesis of four different gold nanostructures namely octahedral, rhombic dodecahedra, truncated ditetragonal prisms and concave cubes by using Ag as seeds [4]. Xia's group too had showed the seed-mediated synthesis of single-crystal gold nanospheres where initial Au seeds were prepared and later it was used to make larger Au nanospheres [5].

Up to now, this seed-mediated growth technique has been widely explored to fabricate nanoparticles with various shapes [6]. However, in most cases, this technique involved two steps where metal seeds such as Ag or Au were firstly prepared followed by second metal ions deposition and reduction on the surface of the metal seeds [7]. It is considered tedious and time consuming. Therefore, in this study, we come up with a single step *in situ* generated seed-mediated growth technique to prepare uniform icosahedral Au@Pd nanoparticles.

In this one-step *in situ* seed mediated growth of Au@Pd nanoparticles, the synthesis was started directly from the source without the initial seeds preparations. We took advantage of the reduction potential difference between Au and Pd to control the rate of reduction of these two salts. As Pd (II) can be reduced faster compared to Au (III), it will form Pd (0) seeds first right before the formation of Au (0) allowing Au (0) to deposit and reduced around the Pd seeds to form Au@Pd nanoparticles. To the best of our knowledge, there has not been an in-depth study on the specific role of Pd in directing Au nanoparticles shape formation.

Another aim of this study is to use a green synthesis method to produce Au@Pd nanoparticles.

Currently, the increasing environmental concerns force scientist to develop and use a greener route to synthesize metal nanoparticles [8, 9]. Methods that employ clean solvents, harmless chemicals, and renewable sources are of utmost important [10]. For example, Nadagouda and co-workers utilized coffee and tea extract to synthesize silver and palladium nanoparticles with size range of 20 to 60 nm [11]. Also, Sujitha *et al.* had successfully reduced $HAuCl_4$ to gold nanoparticles by using citrus fruits juice extract as the reducing and stabilizing agent [12].

In the present work, we report a simple one-pot biofriendly synthesis of Au@Pd bimetallic NPs with controlled morphology using the leaves of *Etlingera Elatior* as the reducing and stabilizing agent. *Etlingera Elatior* (*EE*) also known as "torch ginger" is a plant that belongs to the Zingiberaceae family (the ginger species). It has extensive traditional uses where the young shoots or inflorescences are popular as spices for food flavouring and ornamentals while the leaves are used for wound cleaning [13]. Chan and co-workers [14] reported that of the 26 ginger species screened, leaves of *Etlingera* species had the highest total phenolic content (TPC) and ascorbic acid equivalent antioxidant capacity (AEAC). The high amount of antioxidant content makes *EE* our choice for the biosynthesis of Au@Pd bimetallic NPs.

2. EXPERIMENTS

Materials. Tetrachloroauric (III) acid trihydrate, $HAuCl_4.3H_2O$ (99.5%) and Palladium (II) chloride, $PdCl_2$ were purchased from Merck and Aldrich respectively and were used as received. All aqueous solutions were prepared by using deionized water. Fresh *Etlingera Elatior* leaves were collected from Kuantan, Pahang, Malaysia.

Preparation of Leaf Extract. The *Etlingera Elatior* leaves were washed several times with deionized water to remove any impurities and were allowed to dry for 1 week in room condition. The dried leaves were then grinded and sieved through a 20 mesh sieve. 1 g of *Etlingera Elatior* leaves powder was boiled with 100 ml of deionized water for 10 min. Later, the solution was filtered and stored at 5 ^oC for further experiments.

Biosynthesis of monometallic Palladium and Gold Nanoparticles. 5ml of *Etlingera Elatior* leaves extract was added into the aqueous solution of 15 ml $PdCl_2$ (1 mM) at room temparature. After the completion of bioreduction, the products were collected by repeated centrifuge at 12,000 rpm for 10 minutes and were washed twice with deionized water for characterization. Gold nanoparticles were prepared in the same manner by substituting the aqueous $PdCl_2$ solution by $HAuCl_4$ (1 mM) solutions.

Biosynthesis of bimetallic Au@Pd Nanoparticles. Three sets of bimetallic NPs with different Au to Pd ratio of 10:1, 1:1 and 1:10 were prepared. In brief, for condition 10:1, 3.5 ml of 1 % *EE* leaf extract was added to the 15 ml mixtures of 5 mM $HAuCl_4$ and 0.5 mM $PdCl_2$. The product was washed twice by centrifugation at 12,000 rpm for 10 min using deionized water and collected for characterizations. Later, a well mixed aqueous solution of Au@Pd NPs with other ratios was prepared in a similar manner using the appropriate concentration of Au and Pd salts.

Characterization. The nanoparticles formation was monitored by UV-visible spectrophotometer Shimadzu 2501PC in the range between 400 nm and 1000 nm. FT-IR spectra were recorded on a Fourier Transform Infrared Perkin Elmer 1600 spectrometer in the spectral range of 4000 cm^{-1} to 400 cm^{-1} using potassium bromide (KBr) pressed disk technique. X-ray powder diffraction (XRD) pattern was recorded using Bruker D8 Advance powder diffractometer with a Cu Kα radiation (l = 1.5406 Å) operated at 40 mA and 45 kV. Diffraction patterns were recorded over a 2θ range from 20^0 to 90^0. The morphology of the naoparticles, average particle size and size distribution were determined by TEM-EDS (JEM-2100, 200kV). All electrochemical measurements were performed using EA163 potentiostat. A conventional three electrode cell configuration was used for the voltammetric measurements. The working electrode was a glassy carbon electrode and a silver-silver chloride (Ag/AgCl) as a reference electrode on platinum wire as the auxiliary electrode was employed. All potentials are quoted relative to this reference electrode.

3. RESULTS AND DISCUSSION

Synthesis of monometallic Au & Pd nanoparticles. After mixing the solution of $HAuCl_4$ with the aqueous *EE* leaf extract, the colour of the reaction mixture changed from transparent yellow to ruby red. The observed new colour was attributed to the excitation of surface plasmon vibrations, which directly indicated the formation of Au nanoparticles [15, 16]. This can be proved by the UV-vis analysis in Figure 1 where Au(III) ion solution (Figure 1c) shows no surface plasmon resonance (SPR) absorption, while Au nanoparticles showed SPR band at 536 nm and 723 nm after reduction.

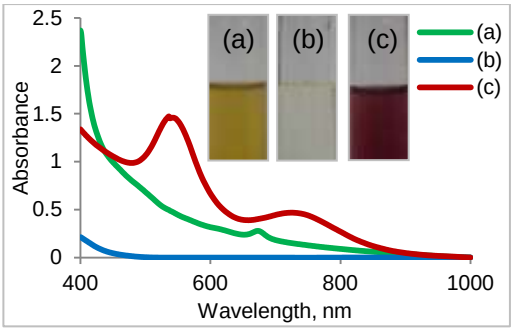

Figure 1 UV-vis spectra of (a) 1% *EE* leaf extract, (b) Au (III) ions and (c) Au nanoparticles.

The absorption band appeared in the visible region in the range between 530 nm and 570 nm is a common feature and is well-known for its surface plasmon resonance (SPR) for Au nanoparticles [17]. Moreover, the SPR peak in this visible region is mostly resulted from the existence of gold nanospheres [18]. The peak around the near IR region between 600 nm and 900 nm is mostly due to gold nanotriangles [19], nanoprism [15, 20], nanoplates [18] or nanorods [21]. The UV-vis spectrum of Au nanoparticles that shows two typical peaks in the visible and IR region was predicted to have mixtures of spherical and anisotropic nanoshapes and was further proved by HRTEM analysis.

HRTEM image in Figure 2 (a-c) elucidate the formation of spherical and anisotropic nanostructures which are mixtures of nanospheres, nanotriangles, nanohexagonal, nanotubes, nanobar and nanodiamonds. The mean size of 200 particles count measured using imej J software was found to be 15.8 ± 6 nm. The distance between atomic planes was measured using fast fourier trasformation (FFT) with d-spacing of 0.237 nm which is in agreement with previous studies [15].

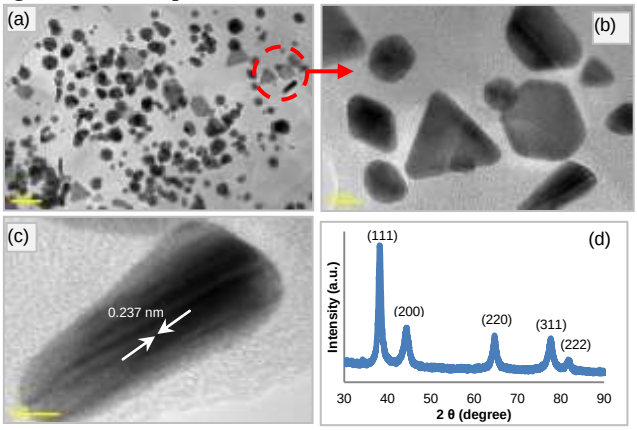

Figure 2 (a-c) TEM images of monometallic Au nanoparticles at different magnifications; (d) XRD patterns of Au nanoparticles.

The XRD pattern in Figure 2d substantiated the formation of crystalline gold nanoparticles. Sharp diffraction peaks can be observed at 38.15°, 44.34°, 64.67°, 77.57° and 81.65° corresponded to (111), (200), (220), (311) and (222) face-centered cubic (FCC) planes of gold respectively [22, 23]. The peak corresponds to the (111) FCC plane obviously shows higher intensity compare to other peaks, indicating that (111) plane is the preferential orientation for the growth of Au nanoparticles [24]. Using Debye-Scherer's equation, the average crystal size of gold could be estimated to be about 11.8 nm.

Figure 3a demonstrates the time intervals for the reduction of Au(III) ions by *EE* leaf extract. An aliquot of the reaction mixture was taken for UV-Vis spectroscopic analysis.

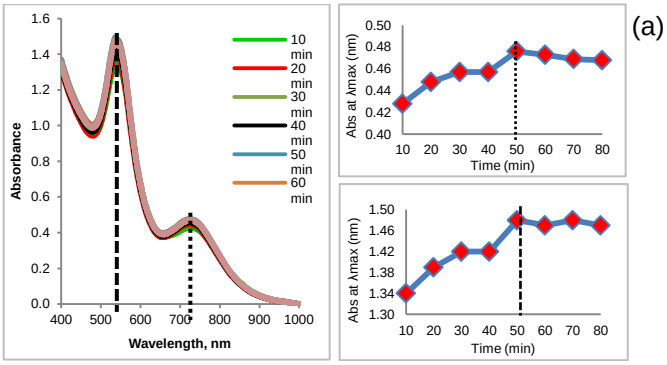

Figure 3 (a) UV-vis spectra of monometallic Au nanoparticles recorded as a function of time; and the plot of absorbance, λ_{max} at (b) 536 nm and (c) 723 nm versus time.

As can be observed, all the spectra exhibit an intense peak at around 536 nm and 723nm corresponding to the SPR of nanocrystalline Au nanoparticles that increases in intensity with time as a result of the continuous bioreduction of Au(III) ions to gold by the *EE* leaf extract [25]. The plot of absorption at λ_{max} versus time of Au^{3+} ion reduction (Figure 3b & 3c) illustrate a rapid bio-reduction of Au(III) ions had occurred and was completed within 50 min which indicate the attainment of saturation in the bio-reduction of metal ions.

In the synthesis of Pd nanoparticles, addition of *EE* leaf extract into the $PdCl_2$ solution resulted in gradual change in colour from yellow to dark brown. The colour change indicated the formation of palladium nanoparticles.

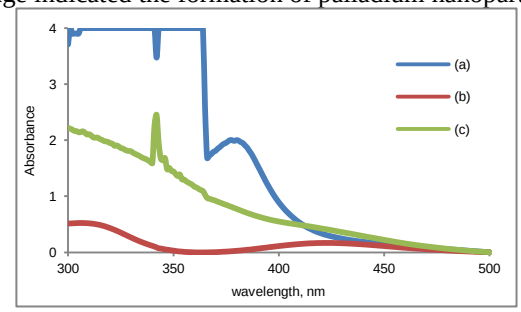

Figure 4 UV-vis spectra of (a) 1% *EE* leaf extract, (b) Pd (III) ions and (c) Pd NPs.

From the UV-vis spectra (Figure 4a), $PdCl_2$ shows absorption peak at 428 nm. After the addition of leaf extracts into the palladium ion solution, this peak disappeared immediately after 10 seconds which proved the reduction of Pd(II) to Pd(0) [26]. The SPR peak of Pd nanoparticles could not be observed due to the small particle size of Pd which is less than 10 nm [1].

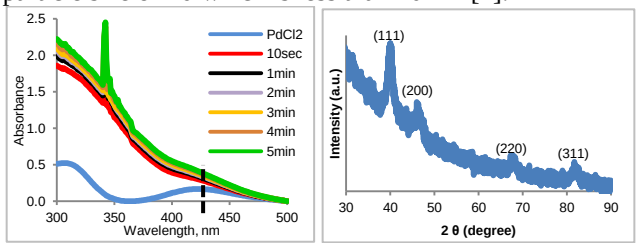

Figure 4 (a) UV-vis spectra of monometallic Pd nanoparticles recorded as a function of time; (b) XRD pattern of Pd nanoparticles.

The crystal structure of Pd nanoparticles was determined using XRD spectroscopy analysis. The XRD diffraction peaks at 39.93 ^{o}, 46.36^{o}, 67.82^{o} and 81.72 ^{o} can be indexed to the (111), (200), (220) and (311) reflections of FCC planes respectively [27, 28]. The mean size of Pd nanoparticles was calculated using the Debye-Scherer's equation which was about 7.7 nm. The small average size of Pd nanoparticles is an evident for the missing SPR peak in the UV-vis spectra.

FTIR analysis was conducted to identify the possible biomolecules which are responsible for the reduction of Au and Pd metal ions, capping and stabilizing of the bioreduced Au and Pd nanoparticles synthesized by the *Etlingera Elatior* leaf extract. The FTIR spectrum of the leaf extract (Figure 5a) showed peaks at 3369 cm^{-1} (O-H group or phenolic compounds), 2924 cm^{-1} (C-H or aldehyde group) 1638 cm^{-1} (C=O group), 1382 cm^{-1} (carboxyl group), 1283 cm^{-1} (C-O group) and 1063 cm^{-1} (aromatic C-C group). All these vibration bands were functional groups of plant extracts which were responsible for the bioreduction of nanoparticles. The presence of the antioxidant compounds like flavanoids, polyphenols, tannis and anthocyanins were reported in the *Etlingera Elatior* leaf extract [13, 29, 30]. The FTIR spectrum of both Au and Pd nanoparticles posed almost the same FTIR spectrum pattern as *Etlingera Elatior* plant extract. The peaks observed for Au nanoparticles (Figure 3.6 b) at 3362 cm^{-1} (O-H group), 2917 cm^{-1} (C-H group), 1375 cm^{-1} (carboxyl group), 1063 cm^{-1} (aromatic ring) suggested the presence of flavanoids or polyphenols adsorbed on the surface of metal nanoparticles. The FTIR spectrum of synthesized Au nanoparticles showed decline in the intensity at 3362 cm^{-1}. This probably suggested the involvement of the phenolic compounds of the leaf extract in the bioreduction process. The spectra in Figure 5 (c) demonstrated peaks at 3407 cm^{-1} (O-H group), 2918 cm^{-1} (C-H group), 1700 cm^{-1} (C=O group), 1375 cm^{-1} (carboxyl group), 1284 cm^{-1} (C-O group), and 1071 cm^{-1} (aromatic ring) which indicated the presence of biomolecules adsorbed on the surface of the Pd nanoparticles. Hence, from the FTIR analysis it was confirmed that the biomolecules from the *Etlingera Elatior* leaf extract acted as capping agents and caused the Au and Pd metal ion reduction to Au and Pd nanoparticles.

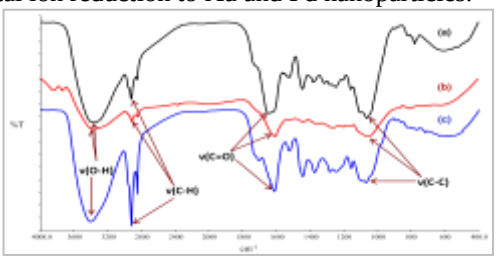

Figure 5 FTIR spectra of (a) *Etlingera Elatior* plant extract, (b) Au nanoparticles and (c) Pd nanoparticles.

By comparing the UV-vis versus time interval of both Au and Pd nanoparticles, the formation of Pd NPs was relatively faster than the formation of Au nanoparticles which was mainly because of the reduction potential difference of the two metal ions [8]. Therefore, cyclic voltametric analysis for both Pd (II) and Au (III) ions were carried out in an aqueous 0.2 M sodium acetate solution on a glassy carbon electrode with scan rate of 50 mVs^{-1} in the potential range of -800 mV to 800 mV at room temparature.

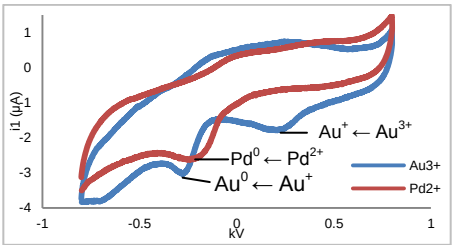

Figure 6 Cyclic voltammograms for (a) Au (III) ions and (b) Pd (II) ions.

Sarvesh Kumar and friends reported that Au (III) will be in favor to reduced first rather than Pd (II) [3], which we believe are vise versa and is proved by the cyclic voltammatric technique. Figure 6a shows the cyclic voltamogram of Au (III) ions where two distinct cathodic peaks were recorded which represents the Au formation in various states [31]. The signal at + 0.227 V was due to the reduction of Au^{3+} to Au^{+}, while the signal at - 0.278 V was the reduction of Au^{+} to Au^{0} forming Au NPs. In contrast, cyclic voltammogram of the Pd NPs showed only one reduction peak at – 0.111 V which is the reduction of Pd^{2+} to Pd^{0} forming Pd NPs. The comparison of both Au (III) and Pd (II) cyclic voltamogram reveals that Pd will form nanoparticles first followed by Au NPs because of its more positive reduction potential of Pd (II). Although the Au (III) signal at + 0.227 V is more positive as compared to the Pd (II) signal at – 0.111 V, gold is still in its ionic form. Whereas, Au (III) ions will form solid Au NPs right after the Pd (II) signal at – 0.278 V. This proved the formation of Pd nanoparticles were comparatively faster than Au NPs.

Synthesis of bimetallic Au@Pd Nanoparticles. Since *EE* leaf extract have the ability to reduce Au and Pd NPs rapidly and effectively, we thought to put Au and Pd NPs together to investigate further in 3 different ratios which are $Au_1@Pd_1$, $Au_{10}@Pd_1$ and $Au_1@Pd_{10}$.

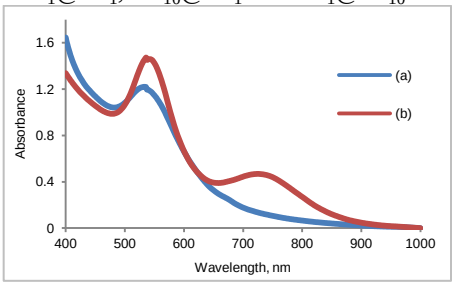

Figure 6 UV-vis analysis of (a) $Au_1@Pd_1$ nanoparticles; (b) Au nanoparticles.

The UV-vis analysis of the one-pot bimetallic $Au_1@Pd_1$ NPs in Figure 7a surprisingly show single absorption peak at 560 nm. The peak near IR region which symbolized the anisotropic nanoparticles had totally vanished, which is attributed to the formation of spherical particles. From the UV- vis result, it is apparent that Pd NPs plays a critical role in the shape control of Au NPs. According to the big difference between the formation time of Au NPs and Pd NPs, our group hypothesized that Pd will form seeds and later Au NPs will slowly grow on the Pd seeds forming Au@Pd bimetallic NPs as display in Scheme 1.

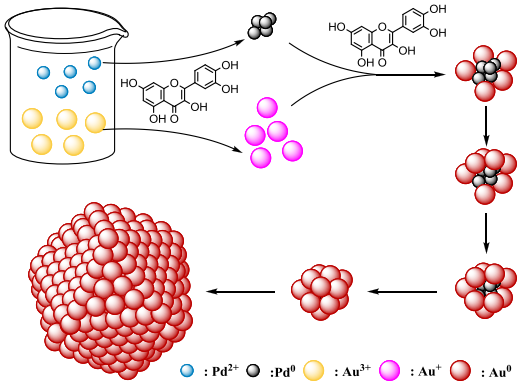

Scheme 1. Schematic diagram of Au@Pd nanoparticles formation.

The HRTEM image in Figure 8 gives evidence that there are only spherical nanoparticles as oppose to the Au monometallic nanoparticles which has too many shapes. Figure 8b shows excess of Pd NPs seeds were formed. The combination of Au and Pd forming bimetallic Au@Pd NPs amazingly control the anisotropic shapes of AuNPs to only nanospheres.

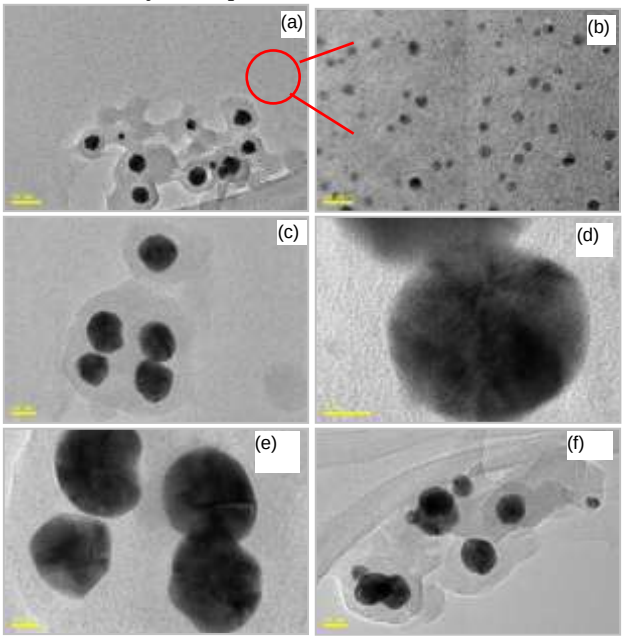

Figure 8 (a-f) TEM images of bimetallic Au-Pd NPs at different magnifications.

EDX was recorded at different spots in Figure 9 to determine the atom % of Pd nanoparticles and Au nanoparticles. Spot 1, 2 and 3 showed higher percentage of Au nanoparticles which is 81 %, 72 % and 78%, respectively as compared to Pd nanoparticles which is 19 %, 28 % and 22 %, respectively. On the other hand, EDX at spot 4 shows almost equal percentage of Au and Pd nanoparticles which is 46 % and 54 %, correspondingly. Spot 1, 2 and 3 read higher percentage of Au nanoparticles as compared to Pd nanoparticles due to the growth of Au around the Pd seeds. Spot 4 have balance or slightly higher amount of Au nanoparticles because Au was just started to gather and grow around the Pd seeds.

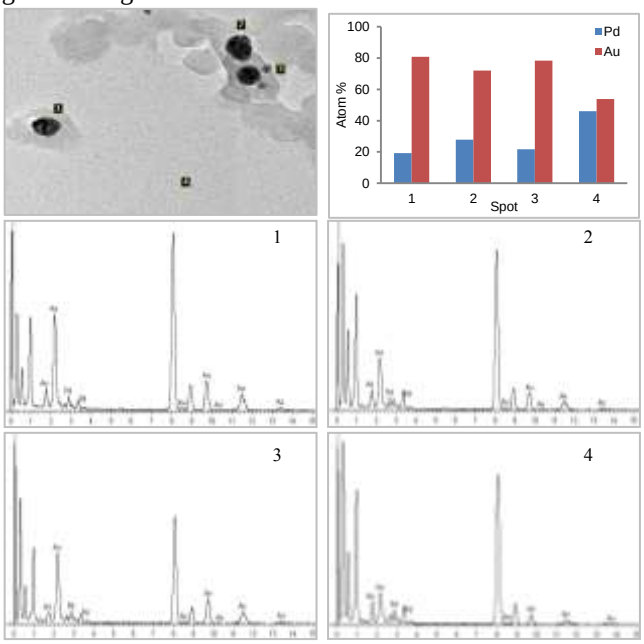

Figure 9 EDX results of Pd NPs and Au NPs atom % taken at spot 1, 2, 3 and 4.

Furthermore, to ascertain the presence of both Au_1-Pd_1 NPs, the composition and the surface valances states of the metals were further derived by XPS measurements (Figure 10). Pd(0) shows a doublet peaks of $3d_{5/2}$ and $3d_{3/2}$ at binding energy (BE) 336.7 eV and 342.5 eV, respectively . The peaks at 83.5 eV and 87.1 eV where the BE are corresponded to the $4f_{7/2}$ and $4f_{5/2}$ valance states of metallic Au [32]. Also, the strong absorption intensity of component O and C observed, clearly indicate the presences of the biocapping agents in the samples.

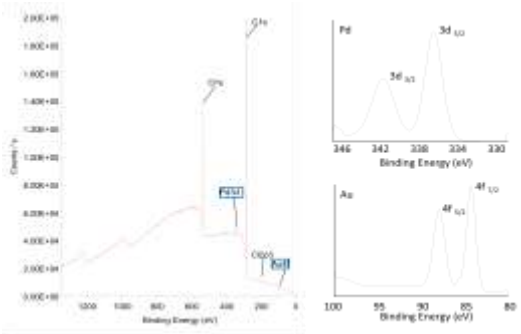

Figure 10 XPS analysis of $Au_1@Pd_1$ nanoparticles.

Figure 11 demonstrates the XRD pattern of Au@Pd nanoparticles with vary ratios. The 2θ values for all three Au@Pd NPs were very similar to monometallic Au NPs. There are no diffraction peaks that can be assigned to Pd for all three Au@Pd NPs. This could be attributed to the small size of Pd and the amorphous nature of Pd [33, 34]. The obvious amorphous peak at 12.9^o for both $Au_1@Pd_1$ and $Au_1@Pd_{10}$ is belongs to the capping and stabilizing agent of *EE* leaf extract.

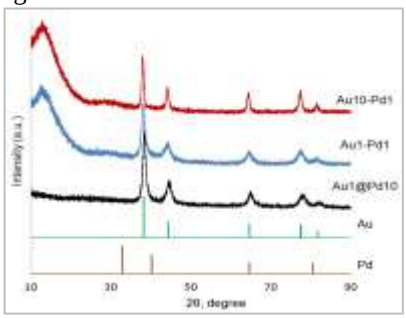

Figure 11 XRD patterns of (a) $Au_1@Pd_1$, (b) $Au_1@Pd_{10}$ and (c) $Au_{10}@Pd_1$

4. CONCLUSION

In conclusion, we have demonstrated the formation of Au@Pd nanospheres with one-step seed-mediated growth process by taking advantage of the reduction potential difference of both metals. The nanoshapes mixtures of Au nanoparticles can be easily controlled by adding Pd in the reaction. This research also reveal that the *Etlingera Elatior* leaf extract is an excellent bioreductant and capping agent which is environmentally-friendly, cost effective and simple for the synthesis of Au and Pd nanoparticles. This green synthesis method eliminates the use of additional chemical stabilizer or capping agents. In addition, FTIR and EDX analyses confirmed that the polyphenolic compounds present in *Etlingera Elatior* leaf extract plays an important role as a reducing and stabiliazing agent.

ACKNOWLEDGMENTS

The authors thank the Ministry of Education Malaysia (MOE) and Universiti Teknologi Malaysia (UTM) for a Research University Grant (vote number 03H06 & 03H81) and to MOE for a scholarship to Wong Sze Ting under the My Brain 15 programme.

REFERENCE

[1] Yujie, X., et al., *Size-Dependence of Surface Plasmon Resonance and Oxidation for Pd Nanocubes Synthesized via a Seed Etching Process.* Nano Letters, 2005. **5**.

[2] Guowu, Z., et al., *Green synthesis of Au–Pd bimetallic nanoparticles: Single-step bioreduction method with plant extract.* Materials Letters, 2011. **65**.

[3] Sarvesh Kumar, S., et al., *Green synthesis of Au, Pd and Au@Pd core–shell nanoparticles via a tryptophan induced supramolecular interface.* RSC Advances, 2013. **3**.

[4] Personick, M., et al., *Shape control of gold nanoparticles by silver underpotential deposition.* Nano letters, 2011. **11**(8): p. 3394-3398.

[5] Zheng, Y., et al., *Seed-mediated synthesis of single-crystal gold nanospheres with controlled diameters in the range 5-30 nm and their self-assembly upon dilution.* Chemistry, an Asian journal, 2013. **8**(4): p. 792-799.

[6] Rice, K.P., A.E. Saunders, and M.P. Stoykovich, *Seed-Mediated Growth of Shape-Controlled Wurtzite CdSe Nanocrystals: Platelets, Cubes, and Rods.* Journal of the American Chemical Society, 2013. **135**(17): p. 6669-6676.

[7] Wang, Y., et al., *Synthesis of Silver Octahedra with Controlled Sizes and Optical Properties via Seed-Mediated Growth.* ACS nano, 2013.

[8] Tamuly, C., et al., *In situ biosynthesis of Ag, Au and bimetallic nanoparticles using Piper pedicellatum C.DC: Green chemistry approach.* Colloids and Surfaces B: Biointerfaces, 2013. **102**(0): p. 627-634.

[9] Kumar, K.M., et al., *Biobased green method to Synthesize Palladium and Iron Nanoparticles using Terminalia chebula Aqueous Extract.* Spectrochimica Acta Part A: Molecular and Biomolecular Spectroscopy, 2012.

[10] Liu, J., et al., *Precise seed-mediated growth and size-controlled synthesis of palladium nanoparticles using a green chemistry approach.* Langmuir, 2009. **25**(12): p. 7116-7128.

[11] Nadagouda, M.N. and R.S. Varma, *Green synthesis of silver and palladium nanoparticles at room temperature using coffee and tea extract.* Green Chemistry, 2008. **10**(8): p. 859-862.

[12] Sujitha, M.V. and S. Kannan, *Green synthesis of gold nanoparticles using Citrus fruits (< i> Citrus limon, Citrus reticulata and Citrus sinensis</i>) aqueous extract and its characterization.* Spectrochimica Acta Part A: Molecular and Biomolecular Spectroscopy, 2012.

[13] Chan, E., Y. Lim, and M. Omar, *Antioxidant and antibacterial activity of leaves of Etlingera species*

(Zingiberaceae) in Peninsular Malaysia. Food Chemistry, 2007. **104**(4): p. 1586-1593.

[14] Chan, E.W.C., et al., *Antioxidant and tyrosinase inhibition properties of leaves and rhizomes of ginger species.* Food Chemistry, 2008. **109**.

[15] Smitha, S.L., P. Daizy, and K.G. Gopchandran, *Green synthesis of gold nanoparticles using Cinnamomum zeylanicum leaf broth.* Spectrochimica Acta Part A: Molecular and Biomolecular Spectroscopy, 2009. **74**.

[16] Philip, D. and C. Unni, *Extracellular biosynthesis of gold and silver nanoparticles using Krishna tulsi (Ocimum sanctum) leaf.* Physica E: Low-dimensional Systems and Nanostructures, 2011. **43**(7): p. 1318-1322.

[17] Cuncheng, L., et al., *Synthesis and optical characterization of Pd–Au bimetallic nanoparticles dispersed within monolithic mesoporous silica.* Scripta Materialia, 2004. **50**.

[18] Weiwei, W., et al., *Two-step size- and shape-separation of biosynthesized gold nanoparticles.* Separation and Purification Technology, 2013. **106**.

[19] Chandran, S., et al., *Synthesis of gold nanotriangles and silver nanoparticles using Aloe vera plant extract.* Biotechnology progress, 2006. **22**(2): p. 577-583.

[20] Mohanan, V.S. and K. Soundarapandian, *Green synthesis of gold nanoparticles using Citrus fruits (Citrus limon, Citrus reticulata and Citrus sinensis) aqueous extract and its characterization.* Spectrochimica Acta Part A: Molecular and Biomolecular Spectroscopy, 2013. **102**.

[21] Babak, N. and A.E.-S. Mostafa, *Preparation and Growth Mechanism of Gold Nanorods (NRs) Using Seed-Mediated Growth Method.* Chemistry of Materials, 2003. **15**.

[22] Suvith, V. and D. Philip, *Catalytic degradation of methylene blue using biosynthesized gold and silver nanoparticles.* Spectrochimica acta. Part A, Molecular and biomolecular spectroscopy, 2014. **118**: p. 526-532.

[23] Suman, T., et al., *The Green synthesis of gold nanoparticles using an aqueous root extract of Morinda citrifolia L.* Spectrochimica acta. Part A, Molecular and biomolecular spectroscopy, 2014. **118**: p. 11-16.

[24] Rajan, A., M. Meenakumari, and D. Philip, *Shape tailored green synthesis and catalytic properties of gold nanocrystals.* Spectrochimica acta. Part A, Molecular and biomolecular spectroscopy, 2014. **118**: p. 793-799.

[25] Mukherjee, P., et al., *Synthesis of uniform gold nanoparticles using non-pathogenic bio-control agent: evolution of morphology from nano-spheres to triangular nanoprisms.* Journal of colloid and interface science, 2012. **367**(1): p. 148-152.

[26] Raut, R., et al., *Rapid biosynthesis of platinum and palladium metal nanoparticles using root extract of Asparagus racemosus Linn.* Advanced Materials Letters, 2013. **4**(8): p. 650-654.

[27] Ashok, B., et al., *Banana peel extract mediated novel route for the synthesis of palladium nanoparticles.* Materials Letters, 2010. **64**.

[28] Sheny, D., D. Philip, and J. Mathew, *Rapid green synthesis of palladium nanoparticles using the dried leaf of< i> Anacardium occidentale</i>.* Spectrochimica Acta Part A: Molecular and Biomolecular Spectroscopy, 2012. **91**: p. 35-38.

[29] Sulaiman, S.F., et al., *Effect of solvents in extracting polyphenols and antioxidants of selected raw vegetables.* Journal of Food Composition and Analysis, 2011. **24**(4): p. 506-515.

[30] Wijekoon, M., R. Bhat, and A.A. Karim, *Effect of extraction solvents on the phenolic compounds and antioxidant activities of bunga kantan (< i> Etlingera elatior</i> Jack.) inflorescence.* Journal of Food Composition and Analysis, 2011. **24**(4): p. 615-619.

[31] Yongprapat, S., S. Therdthianwong, and A. Therdthianwong, *RuO2 promoted Au/C catalysts for alkaline direct alcohol fuel cells.* Electrochimica Acta, 2012. **83**.

[32] Chen, Y., et al., *Formation of monometallic Au and Pd and bimetallic Au–Pd nanoparticles confined in mesopores via Ar glow-discharge plasma reduction and their catalytic applications in aerobic oxidation of benzyl alcohol.* Journal of Catalysis, 2012. **289**: p. 105-117.

[33] Shi, Y., et al., *Au–Pd nanoparticles on layered double hydroxide: Highly active catalyst for aerobic oxidation of alcohols in aqueous phase.* Catalysis Communications, 2012. **18**(0): p. 142-146.

[34] Srivastava, S.K., et al., *Green synthesis of Au, Pd and Au@ Pd core–shell nanoparticles via a tryptophan induced supramolecular interface.* RSC Advances, 2013. **3**(40): p. 18367-18372.